Eur. J. Mineral., 38, 373–382, 2026
https://doi.org/10.5194/ejm-38-373-2026

European Journal of
Mineralogy
Open Access

Yttrotungstite-(Nd), a new mineral species from the Nyakabingo tungsten mine, Kigali, Rwanda

Frédéric Hatert[1], **Simon Philippo**[2], **Pietro Vignola**[3], and **Maël Guennou**[4]

[1]Laboratoire de Minéralogie, Département de Géologie, Université de Liège, Bâtiment B18,
Sart Tilman, 4000 Liège, Belgium
[2]Musée national d'histoire naturelle de Luxembourg, 25 Rue Münster, 2160 Luxembourg, Luxembourg
[3]CNR-Istituto di Geologia Ambientale e Geoingegneria – via Mario Bianco, 9 – 20131 Milano, Italy
[4]Department of Physics and Materials Science, University of Luxembourg, 30 avenue des Hauts-Fourneaux,
6342 Esch-sur-Alzette, Luxembourg

Correspondence: Frédéric Hatert (fhatert@uliege.be)

Received: 26 January 2026 – Revised: 25 April 2026 – Accepted: 2 May 2026 – Published: 7 July 2026

Abstract. Yttrotungstite-(Nd), $NdW_2O_7(OH)(H_2O)$, is a new mineral species discovered in the Nyakabingo tungsten mine, Kigali, Rwanda. The mineral occurs in the oxidized zones of the deposit, where it forms tiny yellow-orange tabular crystals associated with anthoinite and hydrokenoelsmoreite. The crystals are transparent, reach a length of a maximum of 100 µm, and frequently form radiated groups. The dominant form is {010}, and a twinning has been observed parallel to (001). The streak of yttrotungstite-(Nd) is white, the lustre is vitreous, and the mineral is non-fluorescent. The Mohs hardness is 1; the tenacity is brittle; and observed cleavage planes are (010) perfect and (100) and (001) excellent. The calculated density is $6.25\,\mathrm{g\,cm^{-3}}$, and refraction indices are $\alpha = 1.90(2)$ and $\gamma = 2.10(2)$. The mineral is optically biaxial, its optical plane is parallel to (010), and the optical orientation is $X \wedge c = 6°$ and $Z \wedge a = 9°$. Pleochroism is from light yellow (X) to yellow (Z). The empirical formula of yttrotungstite-(Nd), calculated on the basis of 15 positive charges assuming 1 (OH) group and 1 H_2O molecule per formula unit, corresponds to the following: $(Nd_{0.36}Sm_{0.13}Ce_{0.12}Pr_{0.08}La_{0.06}Gd_{0.06}Y_{0.05}Dy_{0.03}Yb_{0.02}Ca_{0.01})_{\Sigma 0.92}(W_{2.02}P_{0.02})_{\Sigma 2.04}O_7(OH)(H_2O)$. The crystal structure was refined in space group $P2_1/m$ to the final R1 value of 0.0362, and the measured unit-cell parameters are $a = 5.8534(3)$, $b = 8.6881(3)$, $c = 7.0488(4)$ Å, $\beta = 105.336(5)°$, and $V = 345.70(3)$ Å^3. The structure of yttrotungstite-(Nd) is characterized by edge-sharing WO_6 octahedra, forming kinked chains parallel to the b axis. The NdO_8 complex polyhedra connect three chains together by sharing edges or corners with adjacent WO_6 octahedra. A view perpendicular to the b axis shows that the NdO_8 and WO_6 polyhedra occur in two different types of planes, stacked parallel to the [−101] direction. Neodymium occurs in a very large eight-coordinated site, which can be described as two tetragonal pyramids sharing one common basal edge and sharing the opposite basal edge with a square. Calculated bond-valence sums are discussed in detail, as well as the Raman spectral results. The species and its name were approved by the Commission on New Minerals, Nomenclature and Classification of the International Mineralogical Association under number IMA 2023-064; its abbreviation is "Ytgs-Nd".

1 Introduction

The crucial importance of tungsten in our modern technologies explains why this element is included in the list of critical raw materials published by the European Union (European Union, 2020). In most geological contexts, only two mineral substances are carrying this rare element: scheelite, $CaWO_4$, and “wolframite”, which designate members of a solid solution between the two species hubnerite, $MnWO_4$, and ferberite, $FeWO_4$.

In the Central African tungsten province, which extends from southwestern Uganda to central Rwanda and eastern Congo, most tungsten-bearing minerals of economic value are constituted by varieties of ferberite (Sahama, 1981). This species generally occurs as black platy crystals, showing a characteristic perfect cleavage plane and crystallizing as a primary phase in mineralized quartz veins. A remarkable variety of ferberite, called “reinite”, forms large pseudo-octahedral crystals without any cleavage plane and shows a dull black colour and an earthy lustre. This unusual variety mainly occurs in the “tungsten belt” of central Rwanda (Goldmann et al., 2013) and is produced by a pseudomorphic replacement of scheelite by ferberite.

In such “reinite” pseudomorphs, numerous late alteration phases occur, mainly consisting of tungsten and iron oxides (Sahama, 1981; Goldmann et al., 2013). The centre of the pseudomorphs is occupied by white earthy masses of anthoinite [$Al(WO_3)(OH)_3$], the latest alteration product of the sequence, but several tungstate species are formed between anthoinite and the rim of ferberite. These species include tungstite [$WO_3 \cdot H_2O$], hydrotungstite and meymacite [polymorphs of $WO_3 \cdot 2H_2O$], hydrokenoelsmoreite [$\square_2W_2O_6(H_2O)$] (previously “ferritungstite” and “alumotungstite”), raspite [$PbWO_4$], mpororoite [$WAlO_3(OH)_3 \cdot 2H_2O$], yttrotungstite-(Ce) [$CeW_2O_6(OH)_3$] (previously “cerotungstite”), and yttrotungstite-(Y) [$YW_2O_6(OH)_3$] (previously “yttrotungstite”).

During a field campaign in Rwanda, the Luxembourgish geologist Paul Antun collected, in 1977, several samples from the famous Nyakabingo tungsten mine, close to Kigali. Those samples were donated to the Natural History Museum of Luxembourg, and its curator, Simon Philippo, discovered the yttrotungstite-(Nd) samples that form yellow-orange bladed crystals associated with anthoinite and hydrokenoelsmoreite.

The mineral, which is the Nd-equivalent of yttrotungstite-(Ce) and yttrotungstite-(Y), has been named in agreement with the nomenclature of the yttrotungstite group. It has been approved by the Commission on New Minerals, Nomenclature, and Classification of the International Mineralogical Association (IMA-CNMNC) under number IMA 2023-064 (Bosi et al., 2023); its abbreviation is “Ytgs-Nd” (Warr, 2021). Holotype samples used for the photographs, for the EMP analyses, and for the X-ray powder diffraction measurements are deposited in the collections of the Natural History Museum of Luxembourg, catalogue number WPA504. Part of the holotype used for the single-crystal X-ray diffraction measurements and for the optical measurements is deposited in the collections of the Laboratory of Mineralogy, University of Liège, Belgium (catalogue number ULG 21981).

2 Occurrence

The sample used for this study was collected in the Nyakabingo tungsten mine, Kigali, Rwanda (latitude 1°52′33″ S, longitude 30°02′36″ E). The region is well-known as an important source of tungsten and was historically called the “Tungsten belt”. The Nyakabingo deposit, located at 10 km NNW of Kigali, is part of the Mezoproterozoic Karagwe-Ankole Belt of Central Africa, a metallogenic province characterized by W- and Sn-bearing quartz veins, as well as by Nb–Ta–Sn-bearing granitic pegmatites (Hulsbosch et al., 2016).

The Nyakabingo deposit is hosted in a sequence showing an alternation of pyritiferous black shales, quartzites, and psammites that were affected by a low-grade greenschist metamorphism (De Clercq et al., 2008; Dewaele et al., 2016). The W-bearing quartz veins were dated by the Ar–Ar method on muscovite, giving an age of 992.4 ± 1.5 Ma, corresponding to the age of the G4 granites that are certainly the source of the W-bearing vein systems (Dewaele et al., 2016). Two different stages of W mineralization were observed, the first one producing scheelite and massive ferberite and the second one producing the ferberite pseudomorphs after scheelite (“reinite”) (Dewaele et al., 2016).

The quartz veins at Nyakabingo contain the major phases of muscovite, feldspar, pyrite, arsenopyrite, and xenotime-group minerals. The economically valuable minerals are ferberite, cassiterite, and molybdenite. During the last meteoric alteration stage, ferberite, feldspar, and pyrite were altered with the formation of clay minerals, iron oxides, and tungsten secondary phases such as tungstite and anthoinite (Dewaele et al., 2016).

Yttrotungstite-(Nd) was found as a secondary mineral occurring in the oxidized zones of the Nyakabingo tungsten deposit. Dewaele et al. (2016) describe, for the type locality, the following minerals in these oxidation zones: ferberite, anthoinite, hydrokenoelsmoreite, meymacite, raspite, yttrotungstite-(Ce), and iron oxides. In our samples that show a honeycomb texture, we identified yttrotungstite-(Nd) as yellow-orange platy crystals, associated with anthoinite and with microcrystalline yellowish hydrokenoelsmoreite octahedra (Fig. 1).

3 Physical and optical properties

Yttrorungstite-(Nd) forms tiny yellow-orange tabular crystals, in association with anthoinite and hydrokenoelsmoreite

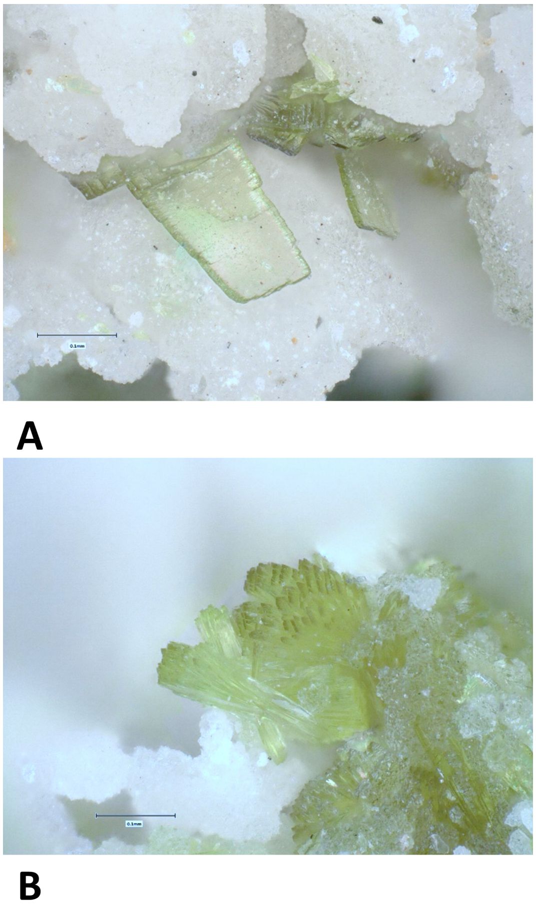

Figure 1. Photographs showing yttrotungstite-(Nd) forming isolated platy crystals **(A)** or fibrous radial aggregates **(B)**, deposited on white micro-crystalline hydrokenoelsmoreite aggregates. The β angle of ca. 105°, between a and c, can be observed on the platy crystal **(A)**, confirming that its main form is $\{010\}$.

(Fig. 1A). The crystals are transparent and reach a length of maximum of 100 µm; they frequently form radiated groups (Fig. 1B). The dominant form is $\{010\}$, and the β angle of ca. 105°, between a and c, is clearly visible on the platy crystals (Fig. 1A). Twinning was observed optically, parallel to (001), in comparison with yttrotungstite-(Ce) (Sahama et al., 1970).

The streak is white, the lustre is vitreous, and the mineral is non-fluorescent. The Mohs hardness is 1 by analogy with the yttrotungstite-(Y) and yttrotungstite-(Ce). Observed cleavage planes are (010) perfect and (100) and (001) excellent; the tenacity is brittle. The density has not been directly determined due to the small size of the crystals and the small amount of available material, but the calculated density is 6.25 g cm^{-3}, obtained from the EMPA data and the single-crystal unit-cell parameters.

Optically, the mineral is biaxial, but the optical sign was impossible to measure due to the orientation of the lamellae parallel to the optical plane. Refraction indices, determined under sodium light ($\lambda = 589$ nm), are $\alpha = 1.90(2)$ and $\gamma = 2.10(2)$. The optical plane is (010), parallel to the lamellae and to the perfect cleavage plane. $X \wedge c = 6°$, $Z \wedge a = 9°$. Pleochroism is from light yellow (X) to yellow (Z).

4 Chemical composition

The chemical composition of yttrotungstite-(Nd) (Table 1) was determined with an electron microprobe at the Department of Earth Sciences "Ardito Desio" in Milano, Italy. The instrument was a Jeol JXA-8200, WDS electron microprobe, using an acceleration voltage of 15 kV, a beam current of 5 nA, and a beam diameter of 3 µm. A total of 17 point analyses were realized, but the water content was not determined due to the small amount of available material. The absence of fluorine in the mineral was confirmed by energy-dispersive X-ray spectrometry (EDS) measurements.

The empirical formula of yttrotungstite-(Nd) was calculated on the basis of 15 positive charges, assuming 1 (OH) group and 1 H_2O molecule per formula unit, according to the structural data (see below). This formula corresponds to the following: $(Nd_{0.36}Sm_{0.13}Ce_{0.12}Pr_{0.08}La_{0.06}Gd_{0.06}Y_{0.05}Dy_{0.03}Yb_{0.02}Ca_{0.01})_{\Sigma 0.92}(W_{2.02}P_{0.02})_{\Sigma 2.04}O_7(OH)(H_2O)$. The simplified formula is $(Nd,Sm,Ce,Pr,La,Gd,Y)W_2O_7(OH)(H_2O)$, and the ideal formula is $NdW_2O_7(OH)(H_2O)$, which requires WO_3 72.99, Nd_2O_3 22.72, and H_2O 4.29, for a total of 100.00 wt %.

5 X-ray diffraction

X-ray powder diffraction data were collected at the University of Liège with a Rigaku Xcalibur four-circle diffractometer used in Debye–Scherrer geometry and equipped with a MoKα radiation source ($\lambda = 0.71073$ Å) and with an EOS charge-coupled device (CCD) detector (Table 2). Unit-cell parameters, refined from the powder data with the LCLSQ program (Burnham, 1991), are as follows: $a = 5.84(1)$, $b = 8.64(1)$, $c = 7.045(8)$ Å, $\beta = 106.1(1)°$, $V = 341.3(6)$ Å^3, $Z = 2$, space group $P2_1/m$.

Single-crystal X-ray diffraction studies were carried out with the same instrument on a crystal of yttrotungstite-(Nd) measuring $0.057 \times 0.088 \times 0.098$ mm. A total of 350 frames with a spatial resolution of 1° were collected by the φ/ω scan technique, with a counting time of 20 s per frame, in the range of $6.00° < 2\theta < 57.70°$. A total of 870 reflections were extracted from these frames, corresponding to 808 unique reflections. The unit-cell parameters refined from these reflections, $a = 5.8534(3)$, $b = 8.6881(3)$, $c = 7.0488(4)$ Å, $\beta = 105.336(5)°$, and $V = 345.70(3)$ Å^3, are in very good agreement with those refined from the X-ray powder diffraction data. Data were corrected for Lorentz, polarization, and absorption effects, the latter with an empirical method using the SCALE3 ABSPACK scaling algorithm

Table 1. Chemical data (in wt %) for yttrotungstite-(Nd) (average of 17 point WDS analyses).

Constituent	Mean	Range	SD (σ)	Reference material	Cation numbers[c]
WO_3	73.40	71.58–74.79	0.96	Pure metal	2.016
MoO_3	0.07	0.00–0.26	0.08	Pure metal	0.003
P_2O_5	0.18	0.08–0.27	0.05	Graftonite (KF16[a])	0.016
As_2O_5	0.04	0.00–0.14	0.05	Realgar	0.002
SiO_2	0.02	0.00–0.05	0.02	Grossular	0.003
TiO_2	0.03	0.00–0.09	0.03	Ilmenite	0.002
Al_2O_3	0.01	0.00–0.02	0.01	Grossular	0.001
CaO	0.09	0.01–0.28	0.07	Grossular	0.010
K_2O	0.01	0.00–0.05	0.01	K feldspar	0.001
Y_2O_3	0.91	0.36–1.45	0.37	Synthetic phosphate[b]	0.051
Ce_2O_3	3.17	2.35–4.49	0.65	Synthetic phosphate[b]	0.123
La_2O_3	1.44	0.68–2.77	0.72	Synthetic phosphate[b]	0.056
Pr_2O_3	2.10	1.61–2.64	0.30	Synthetic phosphate[b]	0.081
Nd_2O_3	9.37	8.90–9.66	0.19	Synthetic phosphate[b]	0.355
Sm_2O_3	3.56	2.39–4.24	0.55	Synthetic phosphate[b]	0.130
Eu_2O_3	0.07	0.00–0.36	0.12	Synthetic phosphate[b]	0.002
Gd_2O_3	1.74	1.04–2.28	0.34	Synthetic phosphate[b]	0.061
Tb_2O_3	0.07	0.00–0.33	0.09	Synthetic phosphate[b]	0.003
Dy_2O_3	0.81	0.57–1.30	0.22	Synthetic phosphate[b]	0.028
Er_2O_3	0.09	0.00–0.25	0.07	Synthetic phosphate[b]	0.003
Yb_2O_3	0.71	0.46–0.90	0.12	Synthetic phosphate[b]	0.023
H_2O[d]$_{\text{calc.}}$	4.24	–	–	–	3.000
Total	102.13				

References for standards: [a] Fransolet (1975) and [b] Jarosewich and Boatner (1991). [c] Cation numbers were calculated on the basis of 15 positive charges. [d] The water content was calculated to reach 1 (OH) group and 1 H_2O molecule per formula unit.

included in the CrysAlisRED package (Oxford Diffraction, 2007). Further details on the structure solution and refinement are given in Table 3.

The crystal structure of yttrotungstite-(Nd) (Figs. 2 and 3) was refined in space group $P2_1/m$. Scattering curves for neutral atoms, together with anomalous dispersion corrections, were taken from the International Tables for X-ray Crystallography, Vol. C (Wilson, 1992). In the final refinement cycle, all atoms were refined anisotropically, leading to the final R1 value 0.0362. Atomic coordinates and site occupancies, as well as equivalent isotropic displacement parameters, are given in Table 4.

The crystal structure is characterized by edge-sharing WO_6 octahedra, forming kinked chains parallel to the *b* axis (Fig. 2). The NdO_8 complex polyhedra connect three chains together by sharing edges or corners with adjacent WO_6 octahedra. A view perpendicular to the *b* axis shows that the NdO_8 and WO_6 polyhedra occur in two different types of planes, stacked parallel to the $[-101]$ direction (Fig. 3).

Neodymium occurs in a very large eight-coordinated site, which can be described as two tetragonal pyramids sharing one common basal edge and sharing the opposite basal edge with a square (Fig. 4). The average Nd–O bond length is

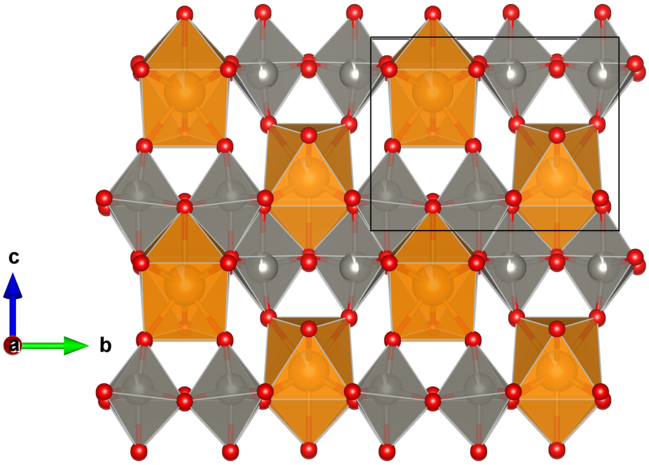

Figure 2. The crystal structure of yttrotungstite-(Nd), viewed perpendicular to the *a* axis. NdO_8 polyhedra are orange, and WO_6 octahedra are grey. Kinked chains, constituted by edge-sharing WO_6 octahedra, are running along the *b* axis. Drawing obtained with the program Vesta (Momma and Izumi, 2011).

Table 2. X-ray powder diffraction data (d in Å) for yttrotungstite-(Nd). Calculated intensities were obtained with the program Vesta (Momma and Izumi, 2011). The eight strongest lines are in bold.

d_{meas}	d_{calc}	I_{meas}	I_{calc}	*hkl*
6.73	6.769	15	25	001
5.62	5.610	10	11	100
4.72	4.704	**100**	**100**	110
3.87	3.829	2	9	101
3.65	3.640	5	13	021
3.30	3.286	**80**	**83**	12-1
3.12	3.112	**20**	**26**	11-2
2.852	2.865	**40**	**18**	121
2.649	2.649	**30**	**38**	031
2.522	2.532	15	14	20-2
2.295	2.301	2	6	131
2.249	2.249	5	1	11-3
2.183	2.183	2	2	013
2.036	2.040	**60**	**18**	23-1
1.829	1.829	**20**	**10**	231
1.775	1.776	10	4	033
1.658	1.657	**20**	**1**	31-3
1.594	1.594	5	3	232
1.575	1.756	5	1	024
1.540	1.538	2	4	052

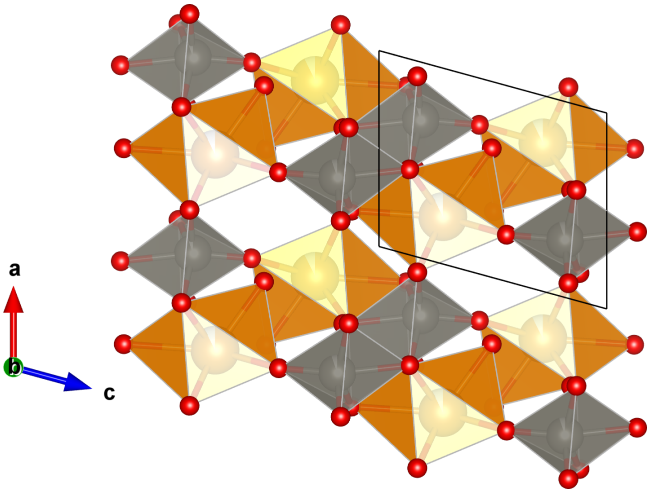

Figure 3. The crystal structure of yttrotungstite-(Nd), viewed perpendicular to the b axis. NdO_8 polyhedra and WO_6 octahedra are located in two different types of planes, stacked parallel to $\{-101\}$. Drawing obtained with the program Vesta (Momma and Izumi, 2011).

2.446 Å, and the average W–O bond length is 1.955 Å (Table 5). The WO_6 octahedron is strongly distorted, with three short bonds (1.764–1.881 Å) and three long bonds (1.961–2.204 Å; Table 5).

Bond-valence sums were calculated for yttrotungstite-(Nd) according to the empirical parameters of Gagné and Hawthorne (2015) (Table 6). Those sums are in fairly good agreement with the ideal values expected for W (5.94) and Nd (3.31), as well as with those expected for the four oxygen atoms O1 to O4 (1.91–2.06). OH5 shows a bond-valence sum very close to the ideal value for an OH group (0.84), and OW6 shows a bond-valence sum of 0.33, indicating that this site is occupied by a water molecule. The end-member formula of yttrotungstite-(Nd) consequently contains one OH group and one water molecule per formula unit and can be written as $NdW_2O_7(OH)(H_2O)$.

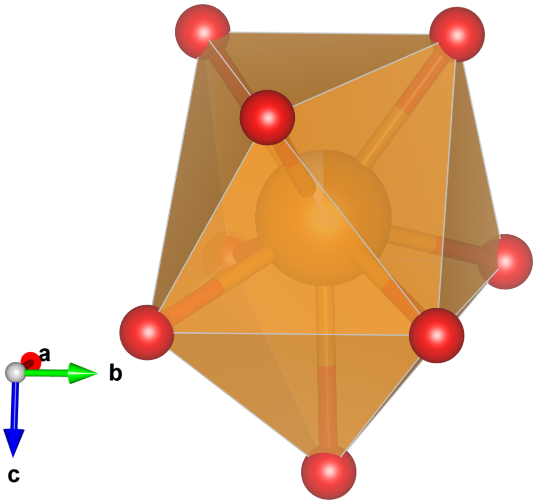

Figure 4. Morphology of the NdO_8 polyhedron in the crystal structure of yttrotungstite-(Nd). Drawing obtained with the program Vesta (Momma and Izumi, 2011).

6 Raman spectroscopy

The Raman spectrum of yttrotungstite-(Nd) (Fig. 5) was recorded at the University of Luxembourg on a Renishaw in-Via micro-Raman spectrometer. The microscope connected to the spectrometer is a Leica equipped with a 50× objective; the working distance was 8 mm. Four wavelengths were used at 785, 633, 532, and 442 nm. The spectra given in Fig. 5 were collected at 633 nm, which offers the best spectral resolution, on four different mineral grains. The laser power was kept at ~ 0.5 mW to avoid any heating effect. The data were collected in three cycles of 30 s exposure with a 1200 g mm^{-1} grating, in a stepwise manner in order to cover the full range up to 4000 cm^{-1}. The Renishaw software Wire 5.1 was used for spectra acquisition. The spectra displayed in Fig. 5 are raw data without any processing, particularly without any baseline correction.

The spectrum is characterized by stretching vibrations of the W–O bonds, occurring between ca. 600 and 1000 cm^{-1}, as well as by stretching vibrations of the OH groups around 3300–3600 cm^{-1}. The absence of peaks at ca. 1600 cm^{-1}, which would correspond to water bending vibrations, is cer-

Table 3. Experimental details for the single-crystal X-ray diffraction study of yttrotungstite-(Nd).

Ideal structural formula	$NdW_2O_7(OH)(H_2O)$
a (Å)	5.8534(3)
b (Å)	8.6681(3)
c (Å)	7.0488(4)
β (°)	105.336(5)
V (Å^3)	345.70(3)
Space group	$P2_1/m$
Z	2
D_{calc} (g cm^{-3})	6.331
Absorption coefficient (mm^{-1})	40.610
$F(000)$	566
Radiation, wavelength (Å)	MoK_α, 0.71073
Crystal size (mm)	0.098 × 0.088 × 0.057
Colour and habit	Yellowish-orange platy
Temperature (K)	293(2)
θ range (°)	3.00–28.85
Reflection range	$-7 \leq h \leq 7$, $-11 \leq k \leq 11$, $-9 \leq l \leq 8$
Total no. of reflections	2462
Unique reflections	870
Unique reflections with $I > 2\sigma(I)$	808
Refined parameters	63
R_1, $F^2 > 2\sigma(F^2)$	0.0362
R_1, all data	0.0392
wR_2 (F^2), all data	0.0876
GOF	1.092
Residuals (e/Å^3)	−2.283, 3.989

Table 4. Atom coordinates and equivalent isotropic displacement parameters (Å^2) for yttrotungstite-(Nd).

	x	y	z	U_{eq}
W1[a]	0.70478(7)	0.06215(4)	0.18298(6)	0.01198(18)
Nd2[b]	0.75846(13)	0.25	0.71977(13)	0.0122(3)
O1	0.7613(14)	0.0878(8)	0.4396(13)	0.0221(19)
O2	0.4358(14)	−0.0654(7)	0.1330(13)	0.0176(18)
O3	0.9225(14)	−0.0744(7)	0.1683(14)	0.022(2)
O4	0.8553(16)	0.25	0.1200(17)	0.018(2)
OH5	0.4453(18)	0.25	0.1556(17)	0.018(2)
OW6	0.3412(19)	0.25	0.505(2)	0.030(3)

[a] Occupancy = 0.945(14) W; [b] occupancy = 0.932(14) Nd.

tainly due to polarization effects. By using the empirical correlation between the wavenumbers of the W–O stretching vibrations and the W–O bond lengths established by Hardcastle and Wachs (1995), it was possible to assign the intense peak at 930 cm^{-1} to the vibrations of the W1–O1 and W1–O3 bonds (calculated wavelengths 900 and 901 cm^{-1}, respectively) and the peaks at 834 and 684 cm^{-1} to the vibrations of the W1–O2′ and W1–O4 bonds (calculated wavelengths 722 and 620 cm^{-1}, respectively). The two long W1–OH5 and W1–O2 bonds (Table 5) produce vibrations around 400 cm^{-1}, but they cannot be accurately attributed to any peak since such long W–O bonds have lost most of their covalency and consequently give rise to weak peaks difficult to assign (Hardcastle and Wachs, 1995).

In the OH-stretching region, five peaks occur that are produced by the vibrations of the OH5 group and of the OW6 water molecule. By using the empirical correlation between the OH-stretching wavenumbers and the O–H…O distances, established by Libowitsky (1999), it is possible to accurately calculate the theoretical wavenumbers corresponding to the O–H…O distances measured in the crystal structure model (Table 5). A comparison of these calculated values with the wavenumbers observed on the Raman spectrum (Fig. 5) indicates that the vibrations of the OH5 groups correspond to

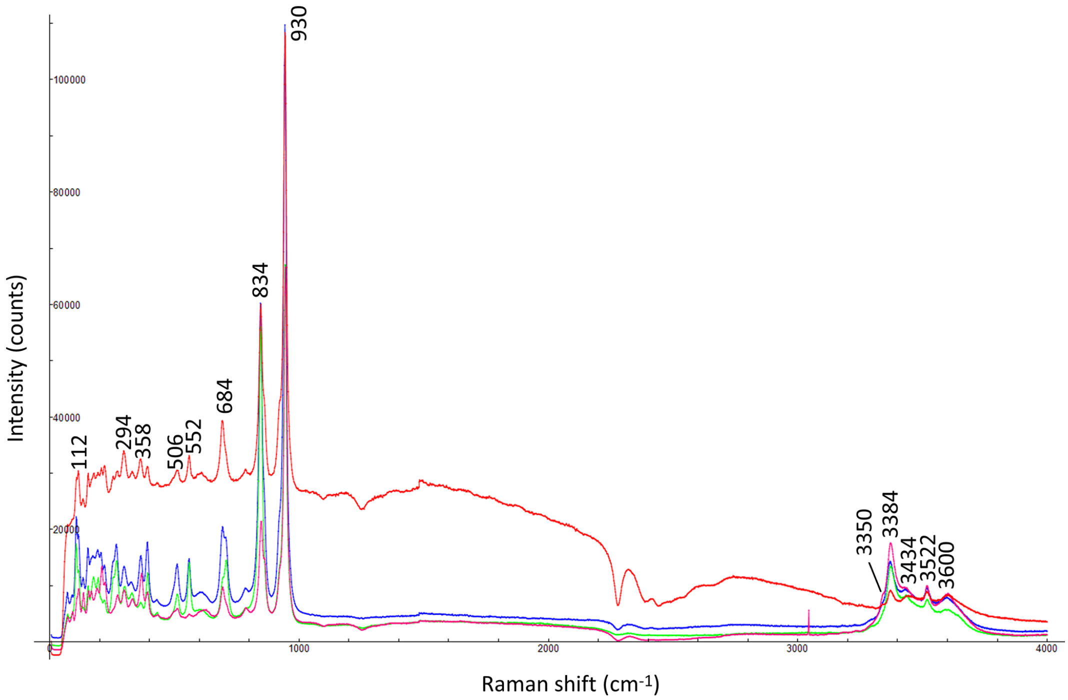

Figure 5. The Raman spectra of yttrotungstite-(Nd), recorded with a laser of 633 nm wavelength. The four spectra correspond to different analysed grains.

Table 5. Selected bond distances (Å) for yttrotungstite-(Nd) and calculated Raman wavelengths (cm^{-1}) corresponding to O–H...O hydrogen bonds.

W1–O1	1.765(9)	Nd2–O1 x2	2.429(8)
W1–O2	2.161(9)	Nd2–O2 x2	2.359(7)
W1–O2’	1.881(7)	Nd2–O3 x2	2.378(7)
W1–O3	1.764(7)	Nd2-O4	2.727(12)
W1–OH5	2.204(6)	Nd2-OW6	2.511(12)
W1–O4	1.961(5)	Mean	2.446
Mean	1.955		
	Observed O–H...O distance	Calculated wavelengths*	Observed wavelengths
OH5–O4	2.481(16)	1472	
OW6–OH5	2.68(2)	3122	
OH5–O1	2.727(12)	3263	3350,
OH5–O2	2.745(7)	3305	3384
OH5–O2’	2.824(14)	3434	3434
OW6–O1	2.974(14)	3541	3522
OW6–O2	3.004(14)	3552	
OW6–O1’	3.041(8)	3561	3600
OW6–O3	3.449(17)	3591	

* Calculated wavelengths were obtained from the empirical correlation established by Libowitzky (1999).

Table 6. Bond-valence table for yttrotungstite-(Nd).

	W1	Nd2	Sum
O1	1.570	0.415 × 2 ↓	1.99
O2	0.476	0.502 × 2 ↓	2.06
O2′	1.086		
O3	1.534	0.477 × 2 ↓	2.01
O4	0.858 × 2 →	0.186	1.90
OH5	0.419 × 2 →		0.84
OW6		0.333	0.33
Sum	5.94	3.31	

the bands at 3350, 3384, and 3434 cm^{-1}, while the vibrations of the OW6 water molecule produce the bands at 3522 and 3600 cm^{-1} (Table 5).

7 Discussion

The new mineral species described in the present paper, yttrotungstite-(Nd), belongs to the yttrotungstite group and is isostructural with yttrotungstite-(Ce) (Sahama et al., 1970) and with yttrotungstite-(Y) (Davis and Smith, 1971). These two species, originally described as “cerotungstite” and “yttrotungstite”, were renamed by Nickel and Mandarino (1987). Yttrotungstite-(Nd) can be numbered in the Strunz classification as 04.FD.20 (Strunz and Nickel, 2002), and its Dana number is 49.03.03.04 (Gaines et al.,

Table 7. Comparison of the physical properties of yttrotungstite-(Nd), yttrotungstite-(Ce), and yttrotungstite-(Y).

Mineral Reference	Yttrotungstite-(Nd) This work	Yttrotungstite-(Ce)[1]	Yttrotungstite-(Y)[2]
Ideal formula	$NdW_2O_7(OH)(H_2O)$	$CeW_2O_7(OH)(H_2O)$	$YW_2O_7(OH)(H_2O)$
Space group	$P2_1/m$	$P2_1/m$	$P2_1/m$
a (Å)	5.8534(3)	5.874(5)	5.77
b (Å)	8.6881(3)	8.700(5)	8.64
c (Å)	7.0488(4)	7.070(5)	6.95
β (°)	105.336(5)	105.45(5)	104.93
Z	2	2	2
Strong X-ray	–	6.83 (36)	6.75(53)
-Lines	-	5.67(3)	5.60(15)
	–	5.08 (14)	4.98(66)
	4.72 (100)	4.75 (9)	4.70(70)
	–	3.87(8)	3.84(25)
	–	3.405 (100)	3.363(100)
	–	3.337(18)	3.269(45)
	3.30 (80)	3.301 (9)	–
	–	3.172(10)	3.137(8)
	3.12 (20)	3.117(14)	3.068(30)
	–	2.892(8)	2.872(34)
	2.852(40)	2.831(10)	2.792(36)
	–	2.668(4)	2.649(25)
	2.649(30)	2.627(17)	2.601(35)
	–	2.273(52)	2.242(48)
	2.036(60)	2.052(5)	2.025(32)
	–	2.012(9)	1.994(18)
	1.829(20)	1.816(3)	1.793(13)
	–	1.767(21)	1.737(19)
	1.658(20)	1.672(9)	1.650(19)
Cleavage	(010) perfect, (100) and	(100) perfect	(010) perfect,
(001) excellent			(10-1) poor
Refraction indices	$\alpha = 1.90(2)$, $\gamma = 2.10$	$\alpha = 1.89$, $\beta = 1.95$, $\gamma = 2.02$	$\alpha = 1.89$, $\beta = 1.98$, $\gamma = 2.02$
Density	6.25 (calc.)	5.82	5.96
Hardness	1	~ 1	~ 1
Colour	Yellow-orange	Orange-yellow	Orange-yellow

[1] Sahama et al. (1970), [2] Davis and Smith (1971).

1997). It corresponds to the unnamed mineral UM2004-//-O:CeHNdSmW, described in the Clara Mine, Wolfach, Germany, by Kolitsch et al. (2004). A comparison of the physical properties of minerals belonging to the yttrotungstite group is given in Table 7. The compatibility index of yttrotungstite-(Nd), according to Mandarino (1981), is 1-(KP/KC) = 0.0583, good (calculated from the density of 6.25 g cm^{-3} obtained from single-crystal unit-cell parameters and electron microprobe analyses).

According to the structural data, the end-member formula of yttrotungstite-(Nd) is written as $NdW_2O_7(OH)(H_2O)$ since the mineral contains one OH group and one water molecule per formula unit. In the yttrotungstite group, however, the formulae of yttrotungstite-(Ce) and yttrotungstite-(Y) were still expressed as $CeW_2O_6(OH)_3$ and $Y(W,Fe,Si,Al,Ti)_2(O,OH,H_2O)_9$ in the IMA-CNMNC list, respectively. Structural data are available for yttrotungstite-(Y) (Davis and Smith, 1971) and by using the atomic coordinates of this species, bond-valence calculations indicate bond-valence sums of 1.13 on the O1 site (which corresponds to our OH5 site) and of 0.31 on the Wat6 site (which corresponds to our OW6 site). These data therefore confirm the presence of one water molecule and one OH group in the structure of yttrotungstite-(Y), thus allowing its formula change to $YW_2O_7(OH)(H_2O)$. The same procedure is applied to the formula of yttrotungstite-(Ce), which becomes $CeW_2O_7(OH)(H_2O)$, in agreement with the uniformization of the yttrotungstite group accepted by the CNMNC (Bosi et al., 2026).

Data availability. All data are available upon request to Frédéric Hatert (fhatert@uliege.be).

Supplement. The supplement related to this article is available online at https://doi.org/10.5194/ejm-38-373-2026-supplement.

Author contributions. The samples investigated herein were discovered in the collections of the MHNLuxemburg by SP, who also took the pictures of the mineral and performed preliminary EDS measurements. Electron microprobe analyses were performed by PV, and the single-crystal and optical measurements were performed by FH, who also handled the CNMNC proposal. MG collected the Raman spectra, and FH wrote the most significant part of the paper.

Competing interests. The contact author has declared that none of the authors has any competing interests.

Acknowledgements. Many thank are due to the reviewers, Fernando Cámara and Ian Grey, for their constructive comments.

Review statement. This paper was edited by Sergey Krivovichev and reviewed by Fernando Cámara and Ian Grey.

References

Bosi, F., Hatert, F., Pasero, M., and Mills, S. J.: IMA Commission on New Minerals, Nomenclature and Classification (CNMNC) – Newsletter 76, Eur. J. Mineral., 35, 1073–1078, https://doi.org/10.5194/ejm-35-1073-2023, 2023.

Bosi, F., Hatert, F., Pasero, M., and Mills, S. J.: IMA Commission on New Minerals, Nomenclature and Classification (CNMNC) – Newsletter 91, European Journal of Mineralogy, in press, 2026.

Burnham, C. W.: LCLSQ version 8.4, least-squares refinement of crystallographic lattice parameters, Department of Earth & Planetary Sciences, Harvard University, 24 pp., 1991.

Davis, R. J. and Smith, G. W.: Yttrotungstite, Mineral. Mag., 38, 261–285, 1971.

De Clercq, F., Muchez, P., Dewaele, S., and Boyce, A.: The tungsten mineralisation at Nyakabingo and Gifurwe (Rwanda): Preliminary results, Geol. Belg., 11, 251–258, 2008.

Dewaele, S., De Clercq, F., Hulsbosch, N., Piessens, K., Boyce, A., Burgess, R., and Muchez, P.: Genesis of the vein-type tungsten mineralization at Nyakabingo (Rwanda) in the Karagwe–Ankole belt, Central Africa, Mineralium Deposita, 51, 283–307, 2016.

European Union: Critical Raw Materials Resilience: Charting a Path towards greater Security and Sustainability, https://eur-lex.europa.eu/legal-content/EN/TXT/?uri=CELEX:52020DC0474 (last access: 14 January 2026), 2020.

Fransolet, A.-M.: *Etude minéralogique et pétrologique des phosphates de pegmatites granitiques*, unpublished PhD thesis, University of Liège, Belgium, 1975.

Gagné, O. C. and Hawthorne, F. C.: Comprehensive derivation of bond-valence parameters for ion pairs involving oxygen, Acta Crystallogr. B, 71, 562–578, 2015.

Gaines, R.V., Skinner, H.C.W., Foord, E.E., Mason, B. and Rozenzweig, A.: Dana's new mineralogy, 8th Edn., John Wiley & Sons, New York, 1819 pp., ISBN 0-471-19310-0, 1997.

Goldmann, S., Melcher, F., Gäbler, H.-E., Dewaele, S., De Clercq, F., and Muchez, P.: Mineralogy and trace element chemistry of ferberite/reinite from tungsten deposits in central Rwanda, Minerals, 3, 121–144, 2013.

Hardcastle, F. D. and Wachs, I. E.: Determination of the molecular structures of tungstates by Raman spectroscopy, J. Raman Spectrosc., 26, 397–405, 1995.

Hulsbosch, N., Boiron, M.-C., Dewaele; S., and Muchez, P.: Fluid fractionation of tungsten during granite-pegmatite differentiation and the metal source of peribatholitic W quartz veins: Evidence from the Karagwe-Ankole Belt (Rwanda), Geochim. Cosmochim. Ac., 175, 299–318, 2016.

Jarosewich, E. and Boatner, L. A.: Rare-earth element reference samples for electron microprobe analysis, Geostand. Geoanal. Res., 15, 397–399, 1991.

Kolitsch, U., Blaß, G., Graf, H.-W., and Gröbner, J.: Neufunde aus der Grube Clara im mittleren Schwarzwald, Lapis, 29, 18–23, 2004.

Libowitzky, E.: Correlation of O-H stretching frequencies and O-H. . . O hydrogen bond lengths in minerals, Monatsh. Chem., 130, 1047–1059, 1999.

Mandarino, J. A.: The Gladstone-Dale relationship: part IV, The compatibility concept and its application, Can. Mineral., 19, 441–450, 1981.

Momma, K. and Izumi, F.: Vesta 3 for three-dimensional visualization of crystal, volumetric and morphology data, J. Appl. Crystallogr., 44, 1272–1276, 2011.

Nickel, E. H. and Mandarino, J.A.: Procedures involving the IMA Commission on New Minerals and Mineral Names and guidelines on mineral nomenclature, Am. Mineral., 72, 1031–1042, 1987.

Oxford Diffraction: CrysAlis CCD and CrysAlis RED, version 1.71, Oxford Diffraction, Oxford, England, 2007.

Sahama, T. G.: The secondary tungsten minerals, a review, Mineral. Rec., 12, 81–87, 1981.

Sahama, T. G., von Knorring, O., and Lehtinen, M.: Cerotungstite, a cerian analogue to yttrotungstite, from Uganda, Bull. Geol. Soc. Fin., 42, 223–228, 1970.

Strunz, H. and Nickel, E. H.: Strunz mineralogical tables, chemical structural mineral classification system, E. Schweitzerbart'sche Verlagsbuchhandlung, Stuttgart, 870 pp., ISBN 3-510-65188-X, 2002.

Warr, L. N.: IMA-CNMNC approved mineral symbols, Mineral. Mag., 85, 291–320, 2021.

Wilson, A. J. C.: International Tables for X-ray Crystallography, Vol. C, Kluwer Academic Press, London, 883 pp., ISBN 0-792-31638-X, 1992.